# THE RESULT OF ELECTRICAL RESISTIVITY INVESTIGATION OF SOLID WASTE LANDFILL CONDUCTED AT NSUKKA MUNICIPALITY USINING ELECTRICAL RESISTIVITY MEASURMENTS

**Abstract**

Solid waste landfill management has been a significant issue for Nigerian urban areas and other developing countries across the globe.Similar to most other cities, Nsukka also generates waste on a daily basis, much of which is dumped in poorly designed and positioned dumping sites. The majority of the disposal sites are found on roadsides, at marketplaces, on farms, and in residential neighborhoods, among other places. The road infrastructure and groundwater are under danger, and the beauty of the impacted communities are not spared. Undoubtedly, the unchecked citation of boreholes as the source of potable water in the majority of our rural and urban communities—given that the government doesn't seem to be providing water to the people—has become a significant challenge.An investigation using electrical resistivity method was conducted around a solid waste dumpsite at Nsukka in Nsukka L.G.A of Enugu State, Nigeria with an aim to investigate the level of groundwater contamination and the objectives to determine the subsurface geoelectric layers, depth to water table, lithology delineation and map out the contamination zones. The scope of this study provides an overview of some of the approaches used to assess the aquifer vulnerability and aquifer potential using Vertical Electrical Sounding (Schlumberger array) and 2D resistivity imaging (Wenner array) in different locations around Nsukka municipality dumpsite. Both methods were used for this study in order to provide a geophysical database for exploration of the study area's groundwater resources and also they are less expensive and less time consuming. VES has proved to be effective in solving groundwater problems in most places in Nigeria (Ezeh and Ugwu, 2010; Ugwu and Ezeh, 2012; Nzemeka*et al.* (2023). Electrical Sounding (VES) and 2D resistivity imaging were carried out with a digital read out resistivity meter (ABEM SAS 1000) to acquire data in the area and were interpreted using the Schlumberger automatic INTERPEX analysis software and the RES2DINV software respectively, which generates model curves using initial layer parameters and display the variations of electrical resistivities respectively. A total of eight (8) sounding and six (6) 2D resistivity imagings were carried out in the area. A contaminant leachate plume was delineated in 2D resistivity sections as low resistivity zones while the VES shows the depth of aquifer. In 2D pseudosections where bluish colours with low resistivities (less than 20.80Ωm) with the depth ranging from 1.28m to 17.1m in the Line 1 and 2 are seen as contaminated zones. The rest of the lines are not contaminated because of their high resistivities (greater than 20.80Ωm). The result of the electrical resistivity survey also showed 4 - 5 layers geo-electric sections and an AA and AK type sounding curves. The VES result shows that VES 1A, 1B, 2A and 2B which are carried out on line 1 & 2 of the wenner lines showed signs of contamination with low resistivity values less than 20.80Ωm complementing the wenner results. The contamination has not yet got to where the aquifer is located on the lines. Since the depth to the aquifer ranges from 30.26m to 155.43m while maximum depth of contamination is 17.1m. It is believed that the leachate has not percolated down to the aquiferous zones as such aquifers are presumed to be free. As such, it

is recommended that boreholes around the study area should not be less than 30m deep to avoid exploiting polluted water.

**Keywords: aquifer, geoelectric section, vertical electrical sounding, Nsukka, borehole, resistivity, 2d resistivity imaging**

## INTRODUCTION

"Landfills are facilities in which solid waste from municipal and industrial sources are disposed.Solid waste landfills (SWL) have become a popular waste management system for the disposal of all manner of waste materials in the municipality. As a result of the imminent impact of solid waste landfills, it has become necessary to investigate the potential for the contamination of soil and groundwater around a municipal solid waste landfill"(Han *et al*., 2013)."Landfill composition is dependent on the type, quantity, composition and source of the solid waste disposed. These waste in Landfills leach out substances when rain falls and percolates through them. The leachate produced can eventually contaminate groundwater" (Pedersen, 1997). "In urban centers, wastes are generated daily and disposed indiscriminately in rivers and landfills without recourse to the environment, local geology and their proximity to the living quarters" Olisah and Obiekezie, (2020). "Wastes, which are described as materials that result from an activity or process but have no immediate economic value or demand and must be discarded, have been managed in a manner that has made the quest of the government to positively actualize the mega city status a difficult task" Nzemeka*et. al.*, (2023). "Ground water in Africa is a very important resource, it provides a reasonable percentage of public water supplies". (IKhifa*et al.*, 2017). "Depending on the composition of the Landfill the underground water may be contaminated by substances like, heavy metals, organic materials and toxic chemicals among others which are leached out of the waste. It is not very easy to purify a ground once it is contaminated. Mills, 1975 noted that effects of some of these contaminants on the biosphere are cumulative or assiduous. Many factors influence the leachate composition including the types of wastes deposited in the landfill, composition of wastes, moisture content, the particle size, the degree of compaction, the hydrology of the site, the climate and the age of the landfill and other site – specific conditions including landfill design and type of liners used, if any" (Leckie *et al*., 1979; Kouzeli – Katsiri*et al*., 1999; Kaur *et al*., 2020).Following a Nigerian adage ''Water is Life'', which means water is a critical factor to life on earth, it is pertinent, and therefore, to understand the groundwater potential in an area, since it is the most reliable and sustainable water source (Singh *et al*. 2018). "Moreso considering groundwater potential geospatial distribution importance to factor of safety anddomestic water supplies for the teeming populace. Furthermore, development especially for residential quarters takes after closeness to and availability of water sources. Following the United Nations Sustainable Development Goals(SDGs), water plays a major role in livelihood (healthcare, poverty and environment); hence, its shortage is always a severe problem to mankind [31]. Understanding the groundwater potential and its development is thus a major factor for economic growth as well as human and environmental health, and poverty reduction. Problems associated with lack of adequate water supply threaten to place the health of people at risk" (Anukam1997).

### Description of the study area

Nsukka is globally known because it plays host to one of the foremost Universities in Nigeria. In view of this, people from different parts of the world are residing there.The study area is located behind Old Ikenga Hotel off UNN- Ezeimo road Nsukka, Nsukka Local Government Area of Enugu State, Southeastern Nigeria. The area lies between longitudes 7°21'6.3"E - 7°22'12.0"E

and latitudes 6°50’4.05”N - 6°50’52.0"N. It spreads over area of about 89.6 $km^2$ as shown in fig. 1. The study area can be accessed through the notable Ezeimo Road off Odenigbo Junction. Nsukka is located in the Northern fringes of Enugu State. It is about 53.5 km North of Enugu Metropolis. Nsukka is situated in Enugu North Senatorial Zone and is notable for hosting the popular University of Nigeria Nsukka. Towns that share a common border with Nsukka are Edem Ani, Alor – uno, Opi, Orba, Ede – Oballa and Obima. Nsukka Local Government Area has an area of 484 $km^2$ (Fig. 2).Before landfilling, the study area was an excavation site and landfilling started in the second quarter of 2011 by open dumping from the hotel management and the residents before it became a permanent dumpsite for Nsukka municipality. Fig 3 shows a part of the dumpsite and its constituents.

The study area consists of three major geologic formations; the Mamu, Ajali and Nsukka formations, respectively. The Mamu Formation, previously known as Lower Coal measures (Reyment, 1965), consists of fine-medium grained, white to grey sandstones, shaley sandstones, sandy shales, grey mudstones, shales and coal seams. “The thickness is about 450m and it conformably underlies the AjaliFormation.TheAjali Formation, also known as False Bedded sandstone, consist of thick friable, poorly sorted sandstones, typically white in colour but sometimes iron-stained. The thickness averages 300 m and is often overlain by considerable thickness of red earth, which consists of red, earthy sands, formed by the weathering and ferroginisation of the formation. The Nsukka Formation, previously known as the Upper Coal measures” (Reyment, 1965; Uma, 2003), lies conformably on the Ajali Sandstone. The lithology is very similar to that of Manu Formation and consists of an alternating succession of sandstone, dark shale and sandy shale, with thin coal seams at various horizons. Eroded remnants of this formation constitute outliers and its thickness averages 250 m.The study area also shows two major types of landforms which comprises of a high relief zone with undulating residual hills, valleys and the lowland areas. The residual hills are the remnants of the Nsukka Formation which constitute the surface layers (Ezeh and Ugwu 2010). These layers are highly weathered and eroded and overlie the Ajali Sandstone.

**Statement of Problems**

Nsukka area is characterized by scarcity, problem of high depth of water table and difficulty in obtaining groundwater. Most people have to trek a very long distance to fetch water from spring-fed stream such as Asho, Ajie, iyi-Nsukka and Ikwoka – Obimo spring which are located at the foot of hills where water is discharged as underground seepage all year round. Also, there are little or no knowledge on the state of environment, depth of water table and level of contaminants in the water table in the study area. Many studies have looked at the depth of aquifer in other places nearby but not at the study area.

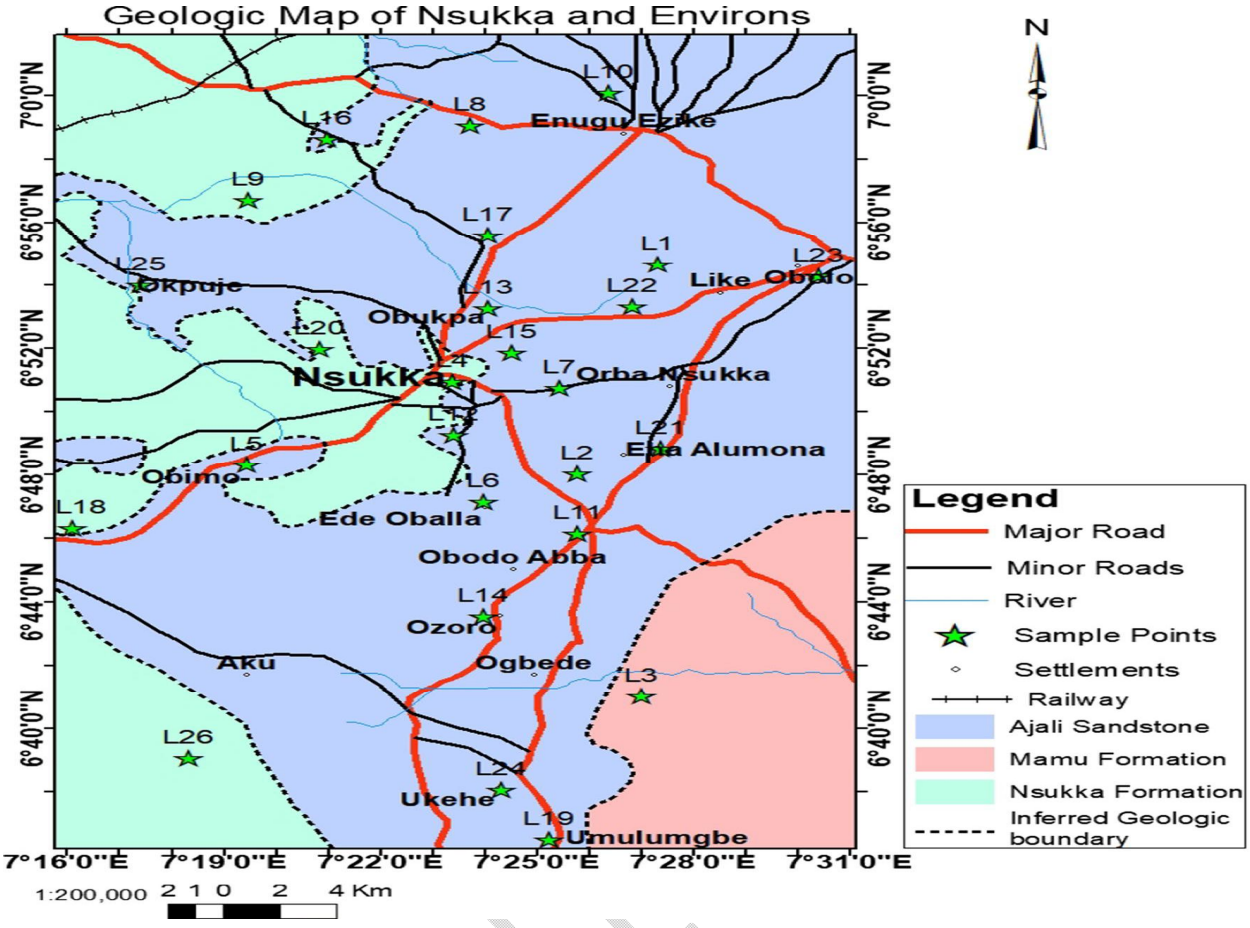


**Fig 1: Geological map of the study area and its environs (Onwe*et al.*, 2022)**

Various workers have studied the effect of solid wastes on the groundwater in Nigeria and all over the world. Raj Kumar, *et. al.*, (2009) applied VES and 2D resistivity imaging to study the rating of municipal solidwaste dumps and landfills as source of groundwater contamination in India. Weiss, *et. al.*, (2008) studied the contamination of soil and groundwater due to stormwater infiltration practices using VES and 2D resistivity imaging.Akpokodje (1999) noted that a staggering amount of solid waste is generated in the Port Harcourt metropolis each year. Aderemi, *et. al.*, (2011) carried out "a preliminary assessment of groundwater contamination by leachate near a municipal solid waste landfill in Lagos and concluded that the leachate generated from the landfill site has a minimal impact on the groundwater quality in the locality". Kadafa, *et. al.*, (2013)studied "the current status of municipal solid waste management practice in FCT Abuja and concluded that municipal solid waste management is a serious issue; due to its human health and environmental sustainability implications that has yet to be properly addressed within the FCT Abuja".Nzemeka*et al.* (2023) assessed "the leachate migration in Nkwelle – Ezunaka Farm Estate, Anambra State using 2D resistivity imaging". VES and 2D resistivity imaging was used to assess the impact of solid wastes on soil and groundwater in Port Harcourt city and its environs (Udom and Esu 2004). Ezeh (2011); Ezeh and Ugwu (2010) used VES to estimate aquifer hydraulic properties and aquifer potential respectively in Enugu State, Nigeria. Onunkwo, *et. al.*, (2014), Abdullahi *et al.*, (2014) and Onwe*et al.*, (2019) applied VES on the comparative analysis of the quality of the shallow and deep aquifer waters of Nsukka and evaluation of groundwater potential and aquifer protective capacity of overburden units around

Opi area in Nsukka respectively. The purpose of this study is to investigate the groundwater contamination in the Nsukka municipality dumpsite.

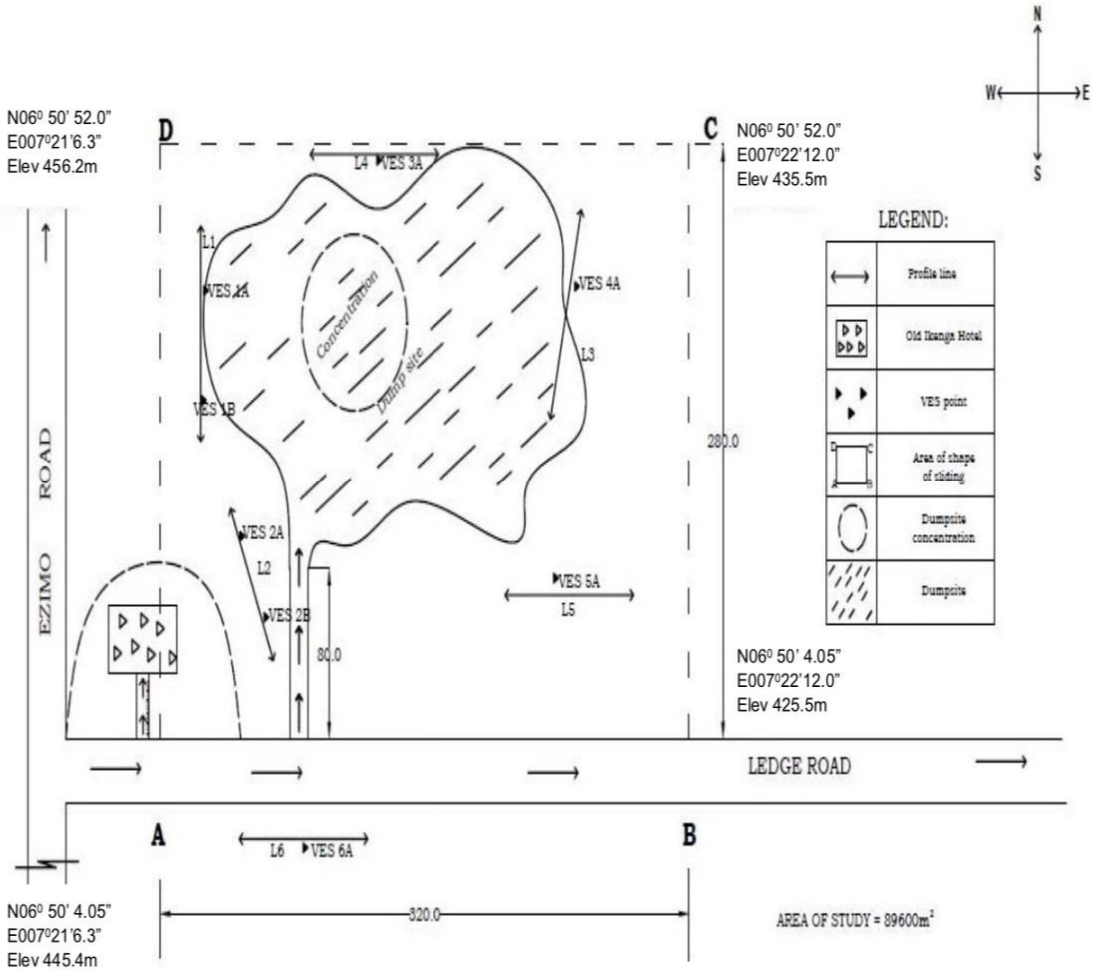


**Fig 2: A sketch map of Nsukka municipality Dumpsite. Source: Authors 2015**

**Fig. 3: Nsukka Municipality Dumpsite showing its surface compositions (Photograph)**

## Methodology

This study involves the use of Vertical Electrical Sounding using Schlumberger array (fig. 5) and 2D resistivity imaging using Wenner array (fig. 6). These method involves the supply of direct current or low-frequency alternating current into the ground through a pair of current electrodes and the measurement of the resulting potential through another pair of electrode called potential electrodes(Obiabunmo*et al.*, 2014). Since the current is known and the potential can be measured, an apparent resistivity can be calculated. For Schlumberger soundings, the apparent resistivity values ($\rho_a$) were plotted against half current electrode separation (AB/2) on a log-log graph and a smooth curve indicative of the vertical distribution in the subsurface was drawn for each of the soundings. Then, the sounding curves were interpreted to determine the true resistivities and thicknesses of the subsurface layers. 2D Resistivity Imaging is a method by which 2D images of subsurface resistivity distribution are generated. Using this method, features with electrical properties differing from those of the surrounding material may be located and characterized in terms of electrical resistivity, geometry and depth of burial. The sounding was used to characterize the various lithologic units and to determine the depth to water table while the resistivity imaging was used to substantiate the result of the sounding as well as to determine the presence of leachate contaminants and the extent of its migration. Both Vertical Electrical Sounding and 2D resistivity imaging are less time consuming and less expensive of all electrical resistivity method. In 2D resistivity imaging, the Wenner array was chosen for this survey because it demands less instrument sensitivity and is good in resolving vertical changes (i.e. horizontal structures), but relatively poor in detecting horizontal changes (i.e. narrow vertical structures). Figure 4 is a schematic illustration of the data processing techniques applied to the raw ER data.



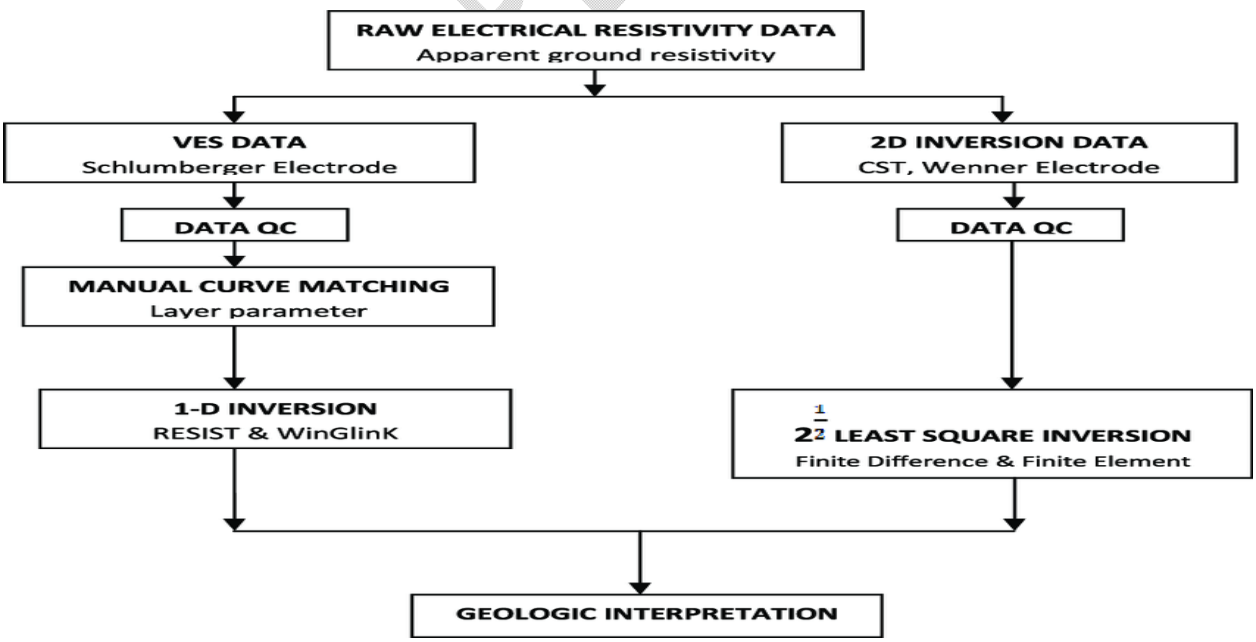


**Fig 4: Flow diagram for Electrical Resistivity data processing Olawale and Olayinka (2012)**

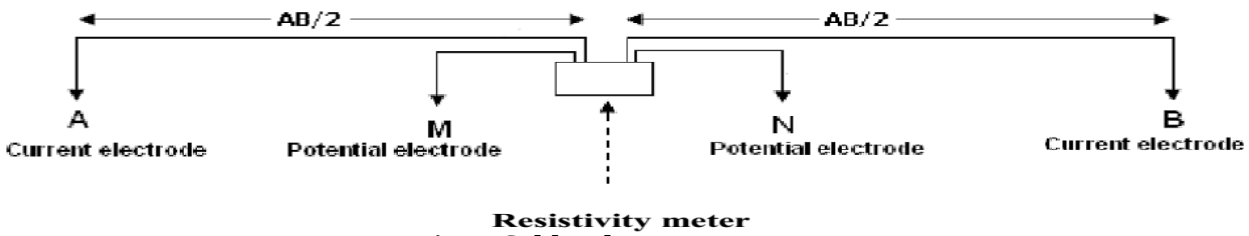


**Fig 5: Schlumberger array**

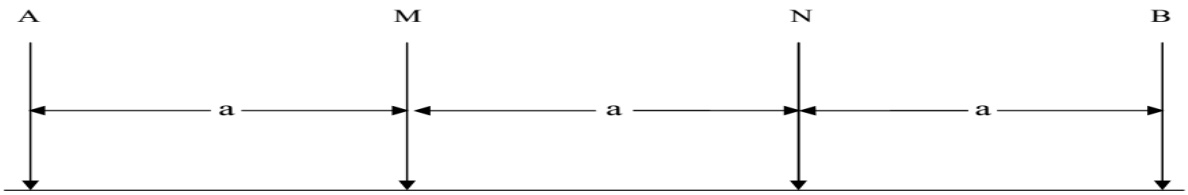


**Fig 6: Wenner array**

A total of eight (8) Vertical Electrical Sounding (VES) using Schlumbeger array and six (6) 2D resistivity imaging using Wenner array were conducted around the dumpsite. The Vertical Electrical Sounding was used to determine the depth of water table and the subsurface geoelectric layers while the 2D resistivity imaging using Wenner array was used to detect and map out the contamination zones around the study area. The ABEM SAS 1000 resistivity meter and the 12 volts battery were placed in the centre of the layout. The two inner electrodes are the potential electrodes while the two outer electrodes are the current electrodes as shown in fig. 5. Four cables were connected to the resistivity meter at the centre of the cable spread and the electrodes were connected at the other end of cables. Current is passedbetween electrodes A and B and monitored by the potential electrodes M and N. As the distance between A and B is increased, deeper horizon have more effect on the potential between M and N. Also when sounding with a Schlumberger array, as distance between the current electrodes are increased, the distance between the current and potential electrodes at the center of the array is also increased. It is this increase between the current and potential electrodes at the center of the array that actually matters in depth probing. The reasonable distance between M and N should be equal or less than one-fifth of the distance between A and B at the beginning. The ratio goes up to one – tenth or one – fifteenth depending on the signal strength. The electrode configuration having a maximum current electrode spread of 600 m was used with a maximum of 300 m on both sides. The current electrode spacing begins with a distance equal to 2 m and extends up to 300 m while the potential electrode spacing begins with a distance of 0.5m and extends up to 20m.The $\frac{AB}{2}$ or half current electrode spacing was increased to a maximum of 300 meters. In most cases $\frac{MN}{2}$ or half potential electrode spacing were overlapping two readings. This means that the potential electrodes were moved only when the potential drops or becomes too small to measure with sufficient accuracy. For the survey, it was not necessary to increase the $\frac{MN}{2}$ distance until the distance $\frac{AB}{2}$ was increased to 9, 75 and 300 meters. At this point, $\frac{\Delta V}{I}$ was measured for both the old and new value of $\frac{MN}{2}$. This procedure permits the detection of near surface inhomogeneities. The data picked from the field was recorded in a data sheet as shown in fig 7.

**VES 1A DATA SHEET**

**STATION NO: VES 1A**

**CO-ORDINATE**
**N: 6°50'66"**
**E: 7°22'0"**
**ELEVATION: 423.4m**
**DATE: 7/6/2015**

| READING NO | $\frac{AB}{2}$ | $\frac{MN}{2}$ | Ka | R (Ω) | $\rho_a$ |
|---|---|---|---|---|---|
| 1 | 2 | | 11.78 | 388.7 | 4578.88 |
| 2 | 3 | 0.5 | 27.50 | 384.1 | 10562.75 |
| 3 | 6 | | 112.36 | 345.8 | 38854.08 |
| 4 | 9 | | 253.79 | 342.5 | 86923.07 |
| 5 | 9 | 2.0 | 60.50 | 30.47 | 1843.43 |
| 6 | 15 | | 173.64 | 19.28 | 3347.77 |
| 7 | 25 | | 487.93 | 14.35 | 7001.79 |
| 8 | 40 | | 1254.00 | 12.81 | 16063.74 |
| 9 | 50 | | 1961.14 | 12.57 | 24651.52 |
| 10 | 75 | | 4416.50 | 10.12 | 44694.98 |
| 11 | 75 | 10.0 | 868.21 | 1.250 | 1085.26 |
| 12 | 100 | | 1555.71 | 14.64 | 22775.59 |
| 13 | 150 | | 3520.00 | 5.563 | 19581.76 |
| 14 | 200 | | 6270.00 | 2.669 | 16734.63 |
| 15 | 300 | | 14127.14 | 0.866 | 12234.10 |
| 16 | 300 | 20.0 | 7040.00 | 0.515 | 3625.6 |
| 17 | 400 | | 12540.00 | | |
| 18 | 500 | | 19611.43 | | |
| 19 | 700 | | 38468.57 | | |

**Fig 7: Sample of VES data sheet**

where
AB/2 is the half current electrode spacing which extends from 2m to 300m on both sides
MN/2 is the half potential electrode spacing which extends from 0.5m to 20m
Ka is the geometric factor (K) calculated using eqn 1which is
$K = \pi(1)$
R (Ω) is the Resistance values collected from the field using ABEM SAS 1000 resistivity meter
$S_a$ is the apparent resistivity values calculated using eqn 2 which is
$S_a = \pi \times R$ (2)

The VES field data were processed using the Schlumberger automatic INTERPEX analysis software, which generates model curves using initial layer parameters by plotting a graph of apparent resistivity against half current electrode spacing (AB/2). From the graph, the number of layers, depth, VES curve and thickness of each layer was deduced. The lithology was inferred to the layers from a standard given by Davis & Annan (1989) as shown in Table 1 and geology of the study areas.

**Table 1: Resistivities of some common rocks and soil (Davis & Annan 1989)**

| Resistivity Range (Ωm) | Soil and Rocks |
|---|---|
| 0 – 30 | Contaminated Lateritic Clay |
| 30 – 50 | Clay |
| 50 – 100 | Shale |
| 100 – 200 | Aquiferous Sandy Shale/Sandy Shale |
| 200 – 600 | Aquiferous Sand/Sand |
| 600 – 1000 | Sandstone |
| 1000 – above | Ironstone/Ferroginized Siltstone |

On the other hand, the 2D resistivity imaging involves the use of Wenner array technique. The Wenner array uses four electrodes equidistant from each other. The outer two electrodes are typically the current (source) electrodes (AB) and the inner two electrodes are the potential (receiver) electrodes (MN) as shown in Fig. 6. A profile line of 100 metres was measured out and the electrodes were moved from the beginning of the profile line to the end of the line with equal electrode spacing "a". The electrode spacing used was 5 m, 10 m, 15 m, 20 m, 25 m and 30 m respectively, the spacing was increased from 5 m to 10 m e.t.c. at the end of the each profile

line.The data picked from the field was presented in a data sheet as shown in fig 7.

**WENNER DATA SHEET FOR PROFILE 1**

**a =5m** **k=31.42** **L=100m**

| X(m) | R(Ω) | $\rho_a$ |
|---|---|---|
| 07.5 | 0.005 | 0.157 |
| 12.5 | 0.268 | 8.427 |
| 17.5 | 0.233 | 7.320 |
| 22.5 | 0.013 | 0.408 |
| 27.5 | 0.035 | 1.099 |
| 32.5 | 0.185 | 5.812 |
| 37.5 | 0.227 | 7.132 |
| 42.5 | 0.037 | 1.162 |
| 47.5 | 0.031 | 0.974 |
| 52.5 | 0.131 | 4.116 |
| 57.5 | 0.080 | 2.513 |
| 62.5 | 0.145 | 4.555 |
| 67.5 | 0.127 | 3.990 |
| 72.5 | 0.385 | 12.096 |
| 77.5 | 0.013 | 0.408 |
| 82.5 | 0.087 | 2.733 |
| 87.5 | 0.067 | 2.105 |
| 92.5 | 0.037 | 1.163 |

**a=10m** **k=62.84**

| X(m) | R(Ω) | $\rho_a$ |
|---|---|---|
| 15 | 0.235 | 14.7674 |
| 20 | 0.159 | 9.99156 |
| 25 | 0.087 | 5.46708 |
| 30 | 0.120 | 7.5408 |
| 35 | 0.137 | 8.60908 |
| 40 | 0.149 | 9.36316 |
| 45 | 0.089 | 5.59276 |
| 50 | 0.045 | 2.8278 |
| 55 | 0.123 | 7.72932 |
| 60 | 0.021 | 1.31964 |
| 65 | 0.067 | 4.21028 |
| 70 | 0.069 | 4.33596 |
| 75 | 0.003 | 0.18852 |
| 80 | 0.001 | 0.06284 |
| 85 | 0.005 | 0.3142 |

**a=15m** **k=94.26**

| X(m) | R(Ω) | $\rho_a$ |
|---|---|---|
| 22.5 | 0.199 | 18.757 |
| 27.5 | 0.221 | 20.831 |
| 32.5 | 0.087 | 8.2006 |
| 37.5 | 0.145 | 13.667 |
| 42.5 | 0.105 | 9.897 |
| 47.5 | 0.167 | 15.741 |
| 52.5 | 0.075 | 7.069 |
| 57.5 | 0.111 | 10.462 |
| 62.5 | 0.200 | 18.852 |
| 67.5 | 2.512 | 236.781 |
| 72.5 | 1.241 | 116.976 |
| 77.5 | 0.842 | 79.366 |

**a=20m** **k=125.68**

| X(m) | R(Ω) | $\rho_a$ |
|---|---|---|
| 30 | 0.081 | 10.180 |
| 35 | 0.061 | 7.666 |
| 40 | 0.031 | 3.896 |
| 45 | 0.115 | 14.453 |
| 50 | 0.113 | 14.201 |
| 55 | 0.061 | 7.666 |
| 60 | 0.027 | 3.393 |
| 65 | 0.029 | 3.644 |
| 70 | 0.085 | 10.682 |

**Fig 8: Sample of Wenner data sheet**

To calculate for the apparent resistivity values, the resistance values obtained from the field was multiplied to the Wenner array's geometric factor given as

$K = 2\pi a$ (3).

Where K is the geometric factor

a is the electrode spacing

The 2D resistivity field data were processed using the RES2DINV inversion software, which subdivides the subsurface into blocks and uses the square inversion to determine the values of each block. The data was first filtered to remove the bad data points whose resistivity values were clearly wrong compared to the neighbouring data points. Least – squares inversion was then carried out on the resistivity data using the RES2DINV software in other to generate the 2D inverse resistivity models.

**Results and Discussion**

The qualitative interpretation of the profile and depth sounding curve were carried out based on distinctive geoelectric parameters on the number of layers represented by the four types of auxiliary curves (A, H, K and Q). The sounding curve is obtained by plotting a graph of apparent resistivity verses half current electrode spacing. The summary of VES interpretation results is shown in Table 3. Out of the eight VES curves VES 1A,1B, 5A, 6A showed AA type of curve while VES 2A, 2B, 3A and 4A showed AK type of curve as seen in Table 2.

**TABLE 2: SUMMARY OF QUALITATIVE INTERPRETATION OF VES CURVES**

| VES | CURVE TYPE | RESISTIVITY PROFILE | NUMBER OF LAYERS |
|---|---|---|---|
| 1A | AA | $\rho_1<\rho_2<\rho_3<\rho_4<\rho_5$ | 5 |
| 1B | AA | $\rho_1<\rho_2<\rho_3<\rho_4$ | 4 |
| 2A | AK | $\rho_1<\rho_2<\rho_3<\rho_4>\rho_5$ | 5 |
| 2B | AK | $\rho_1<\rho_2<\rho_3<\rho_4>\rho_5$ | 5 |
| 3A | AK | $\rho_1<\rho_2<\rho_3>\rho_4$ | 4 |
| 4A | AK | $\rho_1<\rho_2<\rho_3>\rho_4$ | 4 |
| 5A | AA | $\rho_1<\rho_2<\rho_3<\rho_4$ | 4 |
| 6A | AA | $\rho_1<\rho_2<\rho_3<\rho_4<\rho_5$ | 5 |

VES 1A, 2A, 2B and 6A showed 5 geoelectric layers while the others only had 4 geoelectric layers.

The stations were represented and interpreted as VES 1A to 6A as shown in Table 2. VES 1A and 1B were carried out at 25m and 75m respectively on profile 1. The same also goes with 2A and 2B but 3A to 6A were carried out at 45m mark of their respective profiles. The aquiferous sand and aquiferous sandy shale constitutes the aquifer unit with depth ranging from 30.26m to 155.43m as seen in figs 9 - 16. Table 3 shows the summary of VES interpretation result as seen in figs 9 – 16.

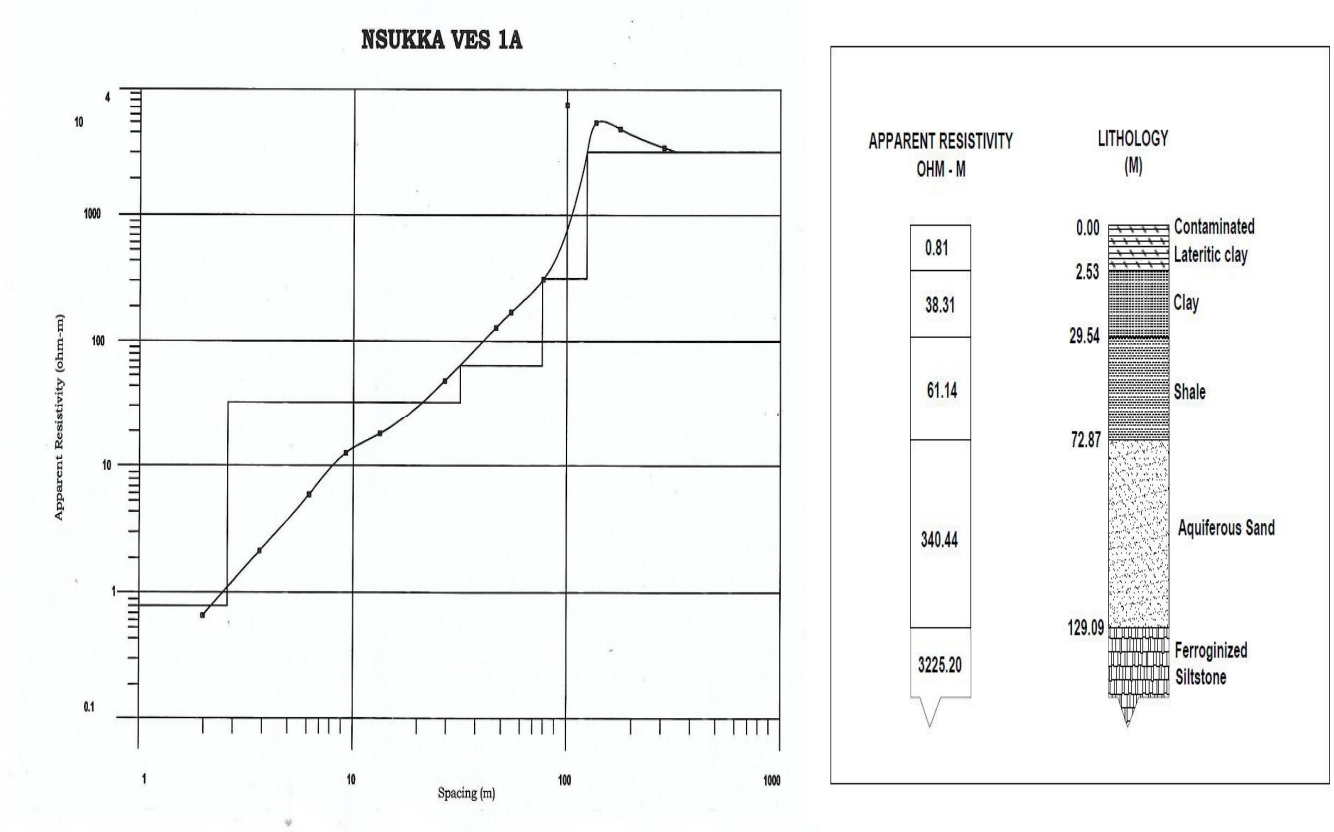


**Fig 9: Interpretation result of VES 1A data**

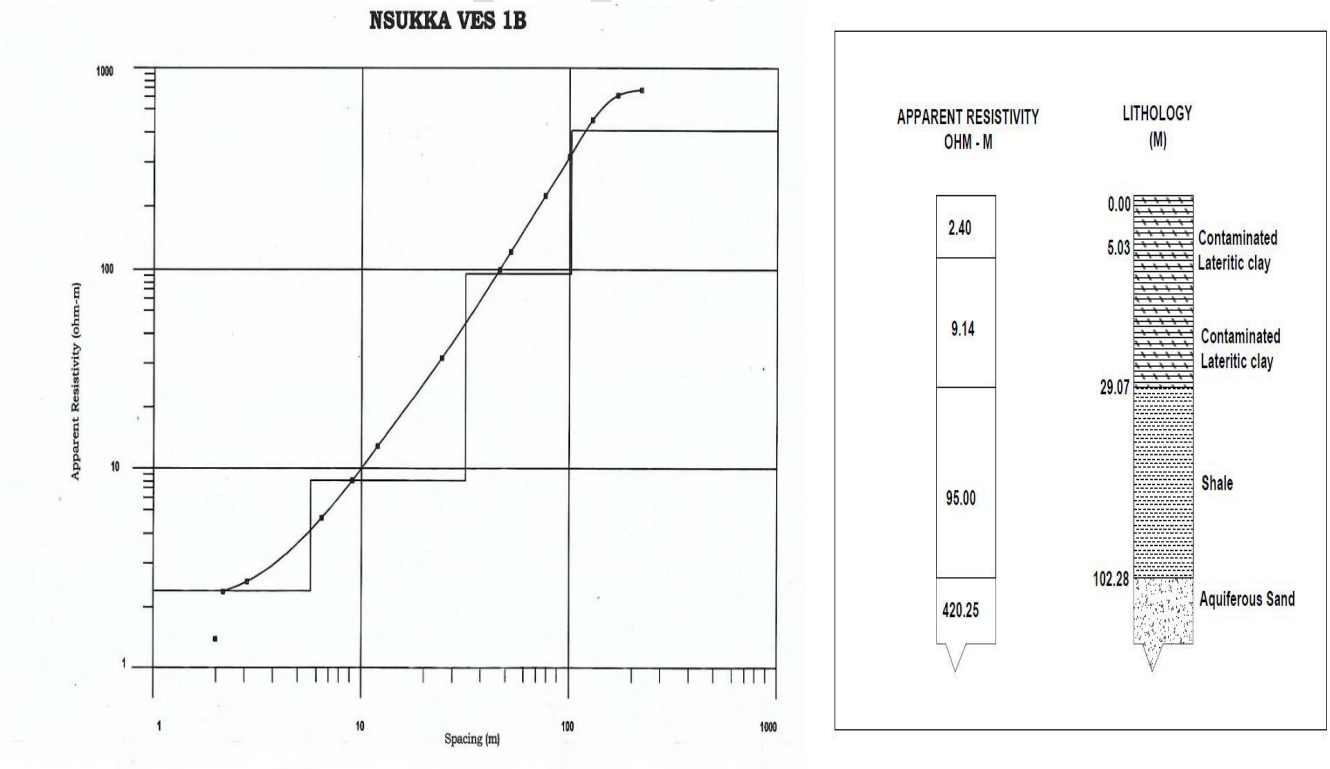


**Fig 10: Interpretation result of VES 1B data**

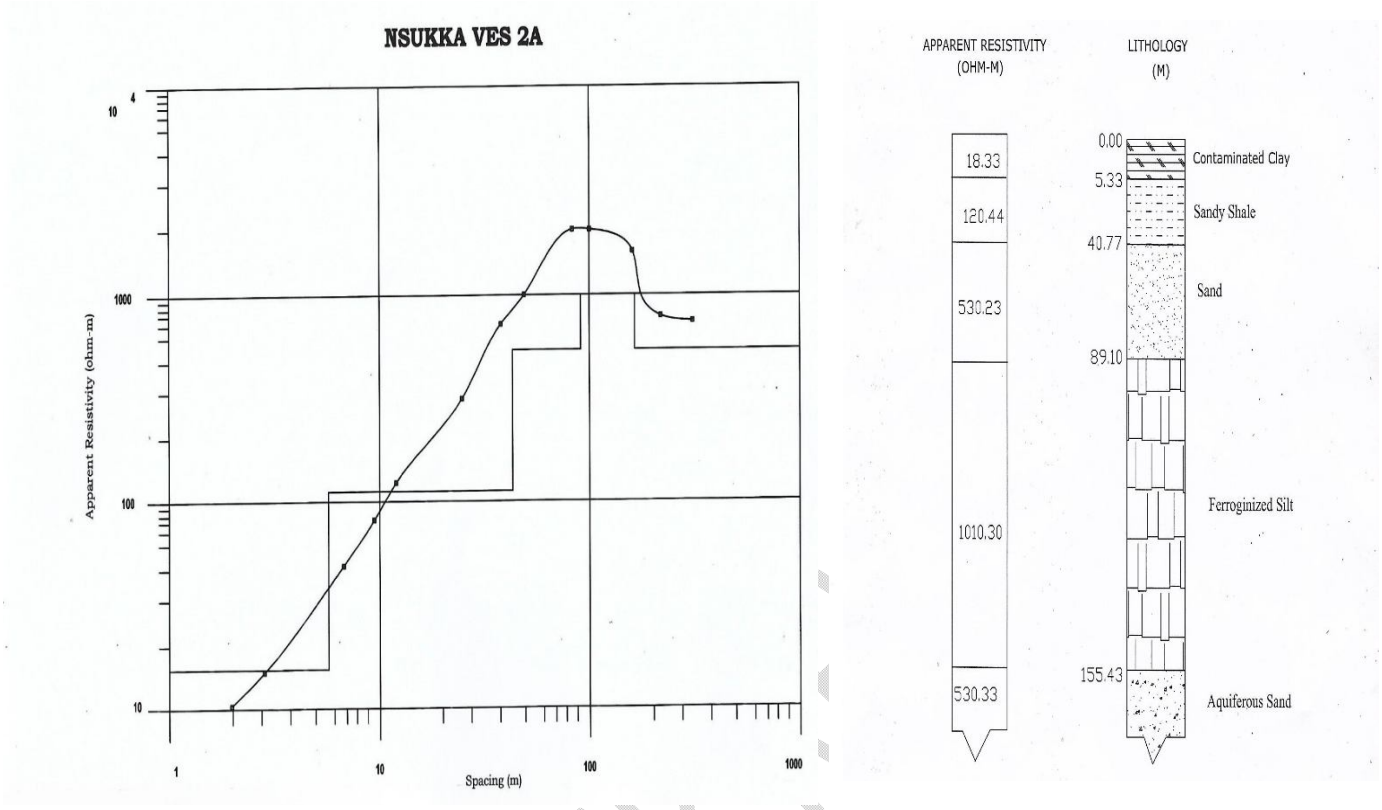


**Fig 11: Interpretation result of VES 2A data**

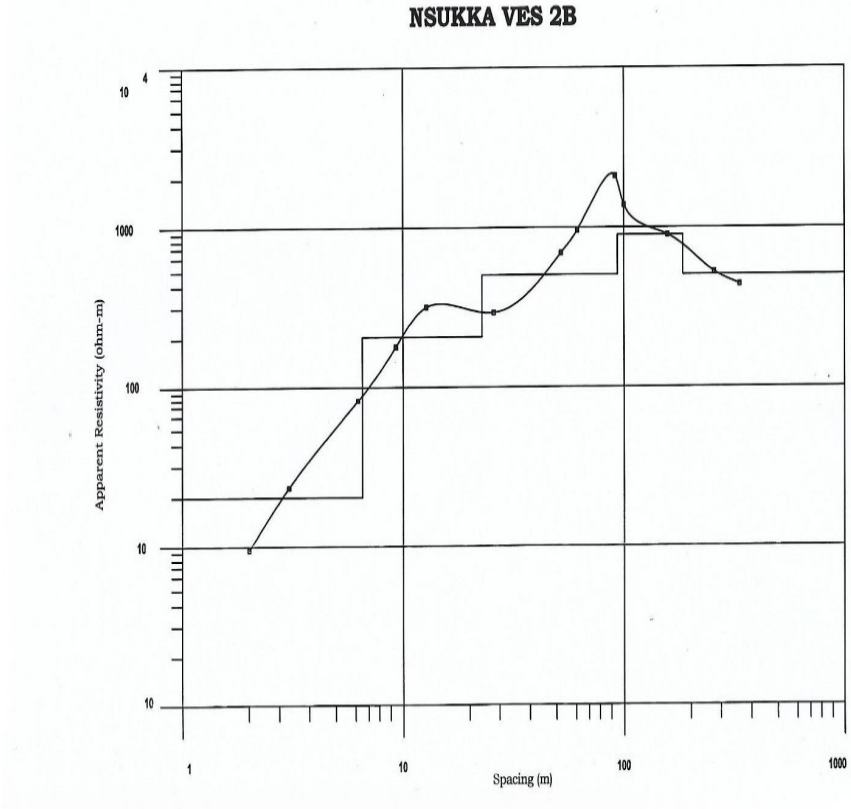


**Fig 12: Interpretation result of VES 2B data**

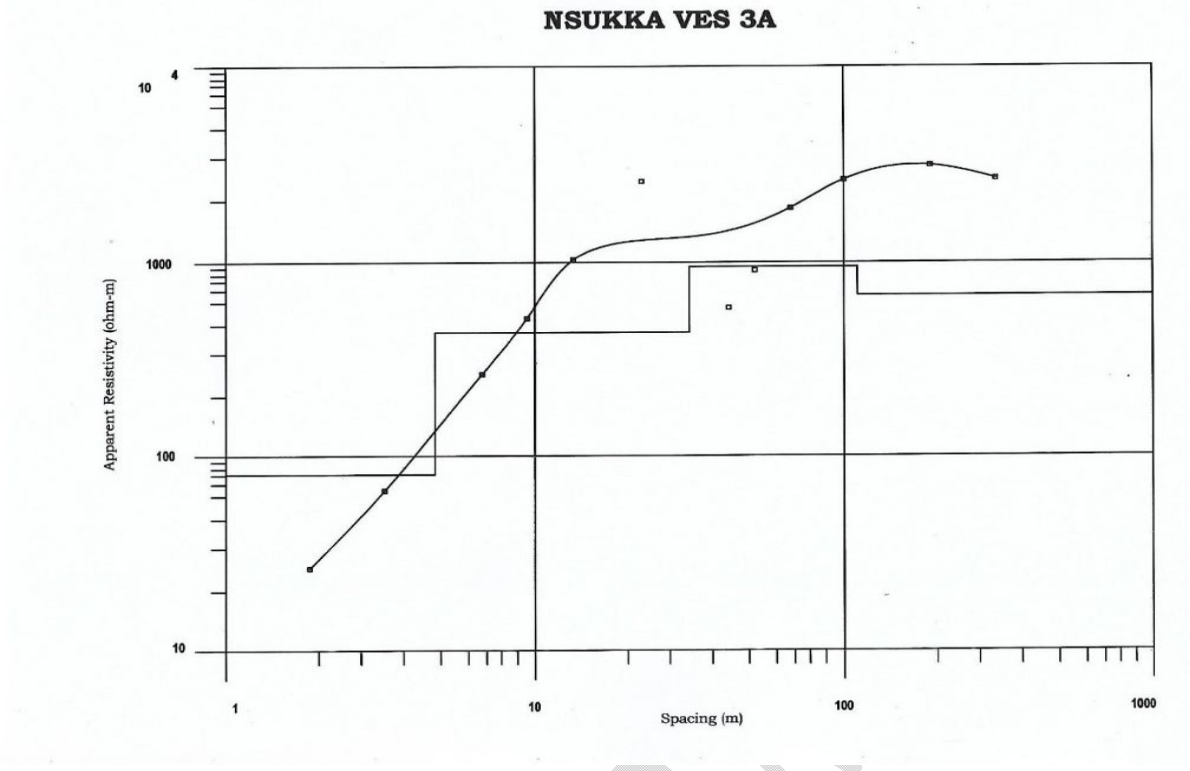


**Fig 13: Interpretation result of VES 3A data**

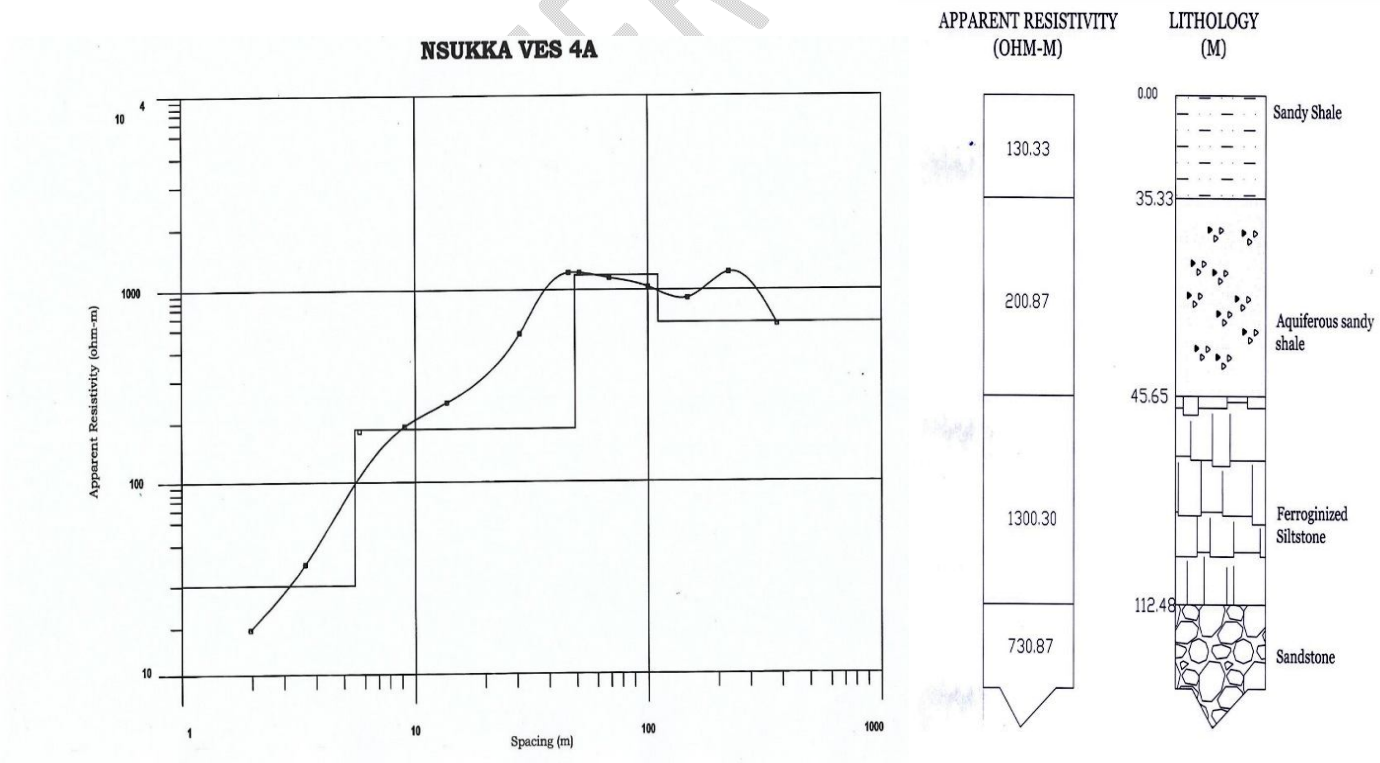


**Fig 14: Interpretation result of VES 4A data**

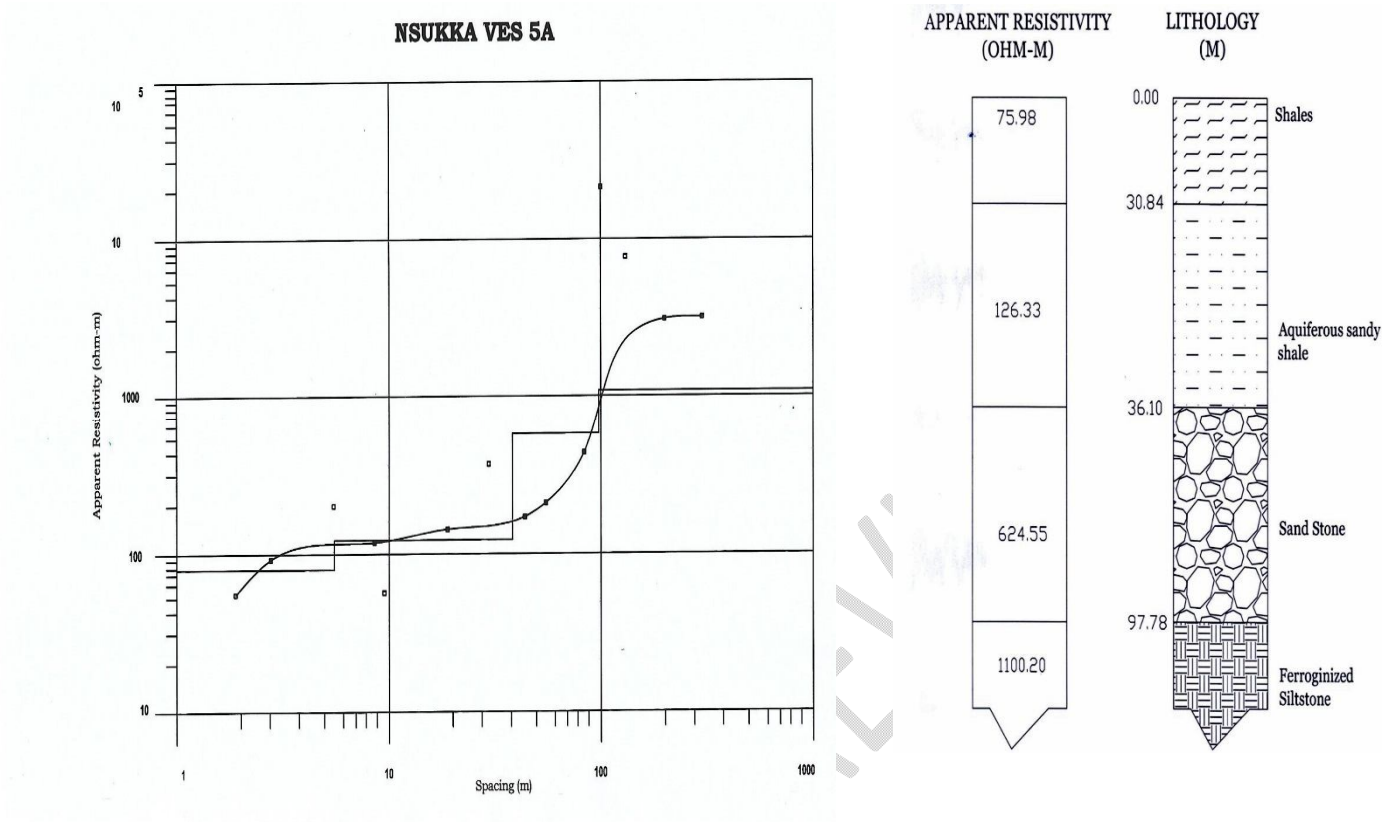


**Fig 15: Interpretation result of VES 5A data**

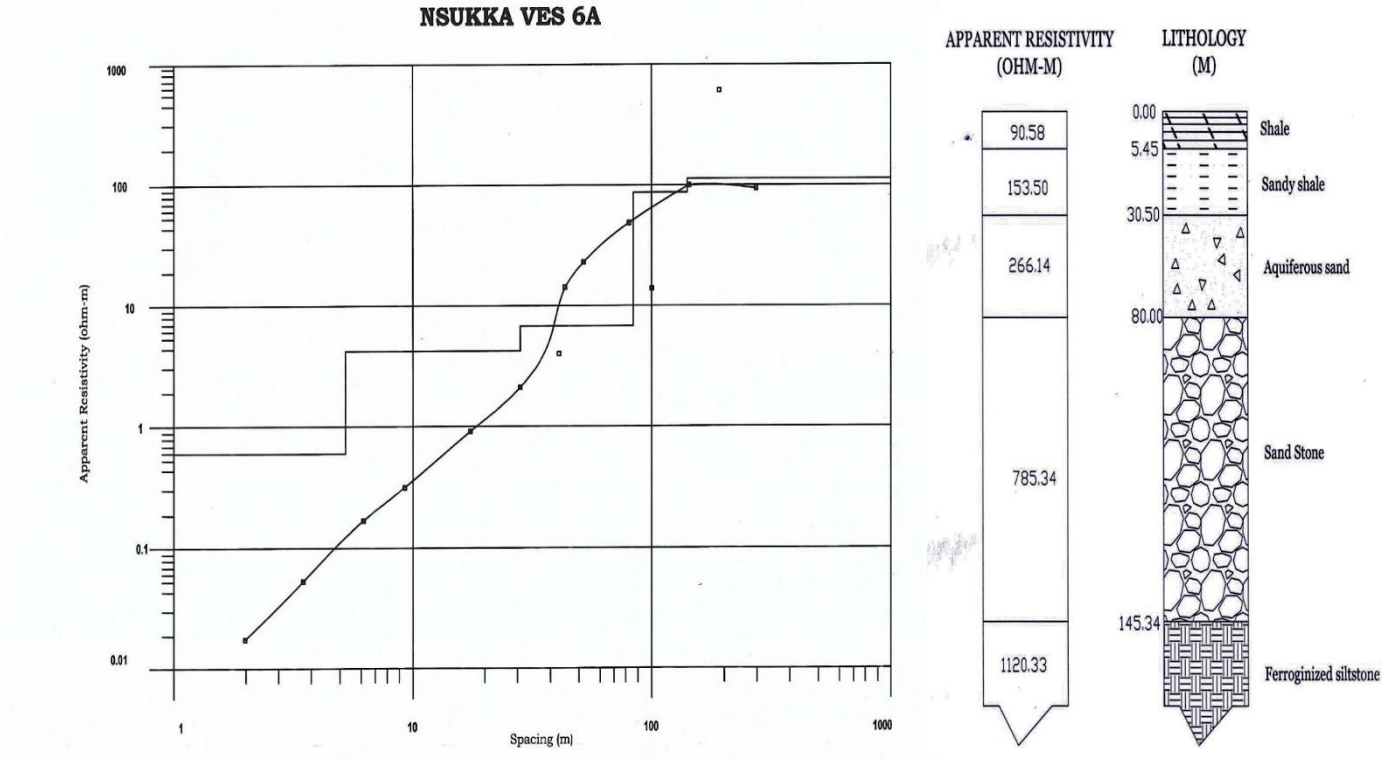


**Fig 16: Interpretation result of VES 6A data**

**TABLE 3: SUMMARY OF VES INTERPRETATION RESULTS**

| VES | Layers | Resistivity (Ωm) | Thickness(m) | Depth (m) | Lithology | Curve type |
|---|---|---|---|---|---|---|
| 1A | 1 | 0.81 | 2.53 | 2.53 | Contaminated lateritic clay | AA |
| | 2 | 38.31 | 27.00 | 29.53 | Clay | |
| | 3 | 61.14 | 43.33 | 72.86 | Shale | |
| | 4 | 340.44 | 56.22 | 129.08 | Aquiferous sand | |
| | 5 | 3225.40 | - | - | Ferroginizedsiltsone | |
| 1B | 1 | 2.40 | 5.03 | 5.03 | Contaminated lateritic clay | AA |
| | 2 | 9.14 | 24.03 | 29.07 | Clay | |
| | 3 | 95.00 | 73.21 | 102.28 | Shale | |
| | 4 | 420.25 | - | - | Aquiferous sand | |
| 2A | 1 | 18.33 | 5.33 | 5.33 | Contaminated lateritic clay | AK |
| | 2 | 120.44 | 35.44 | 40.77 | Sandy shale | |
| | 3 | 530.23 | 48.33 | 89.10 | Sand | |
| | 4 | 1010.30 | 66.33 | 155.43 | Ferroginized siltstone | |
| | 5 | 530.33 | - | - | Aquiferous sand | |
| 2B | 1 | 20.21 | 6.54 | 6.54 | Contaminated lateritic clay | AA |
| | 2 | 196.40 | 35.31 | 41.85 | Sandy clay | |
| | 3 | 460.15 | 68.91 | 110.76 | Aquiferous sand | |
| | 4 | 900.34 | 77.44 | 188.20 | Sandstone | |
| | 5 | 440 | - | - | Aquiferous sand | |
| 3A | 1 | 71.94 | 30.26 | 30.26 | Shale | AK |
| | 2 | 369.40 | 46.49 | 76.75 | Aquiferous sand | |
| | 3 | 948.86 | 69.78 | 146.53 | Sandstone | |
| | 4 | 640.44 | - | - | Sandstone | |
| 4A | 1 | 130.33 | 5.33 | 5.33 | Sandy shale | AK |
| | 2 | 200.87 | 40.32 | 45.65 | Aquiferous sand | |
| | 3 | 1300.30 | 66.83 | 112.48 | Ferroginized siltstone | |
| | 4 | 730.87 | - | - | Sandstone | |
| 5A | 1 | 75.98 | 5.84 | 5.84 | Shale | AA |
| | 2 | 126.33 | 30.26 | 36.10 | Aquiferous sandy shale | |
| | 3 | 624.55 | 61.69 | 97.78 | Sandstone | |
| | 4 | 1100.20 | - | - | Ferroginized siltstone | |
| 6A | 1 | 90.58 | 5.45 | 5.45 | Shale | AA |
| | 2 | 153.50 | 25.05 | 30.50 | Sandy shale | |
| | 3 | 266.14 | 49.50 | 80.00 | Aquiferous sand | |
| | 4 | 785.34 | 65.34 | 145.34 | Sandstone | |
| | 5 | 1120.33 | - | - | Ferroginized siltstone | |

## FIELD RESULTS AND DISCUSSION FOR WENNER

The electrical resistivity images of the earth's subsurface obtained in the study area are presented in Fig. 17 - 22. The results of the Interpreted 2D Electrical resistivity data are presented in a colour coded format consisting of the Inverted 2D Resistivity structure. The RMS obtained for the inverse models range from 3.2 - 7.8%. There is a good correlation between the subsurface images depicted by the models. The horizontal scale on the section is the lateral distance while the vertical scale is the depths which are both in meters. The resistivity models shown were obtained by the optimization technique of RES2DINV by minimizing the difference between the calculated and measured pesudeosections of the apparent resistivity data sets in unison with the result of Kumar *et. al.,* (2009) and Udom*et. al.,* (1999). This is done by plotting apparent resistivity against the pseudo-depth. The contaminated zone resistivities ranges from 0 – 20.8Ωm.

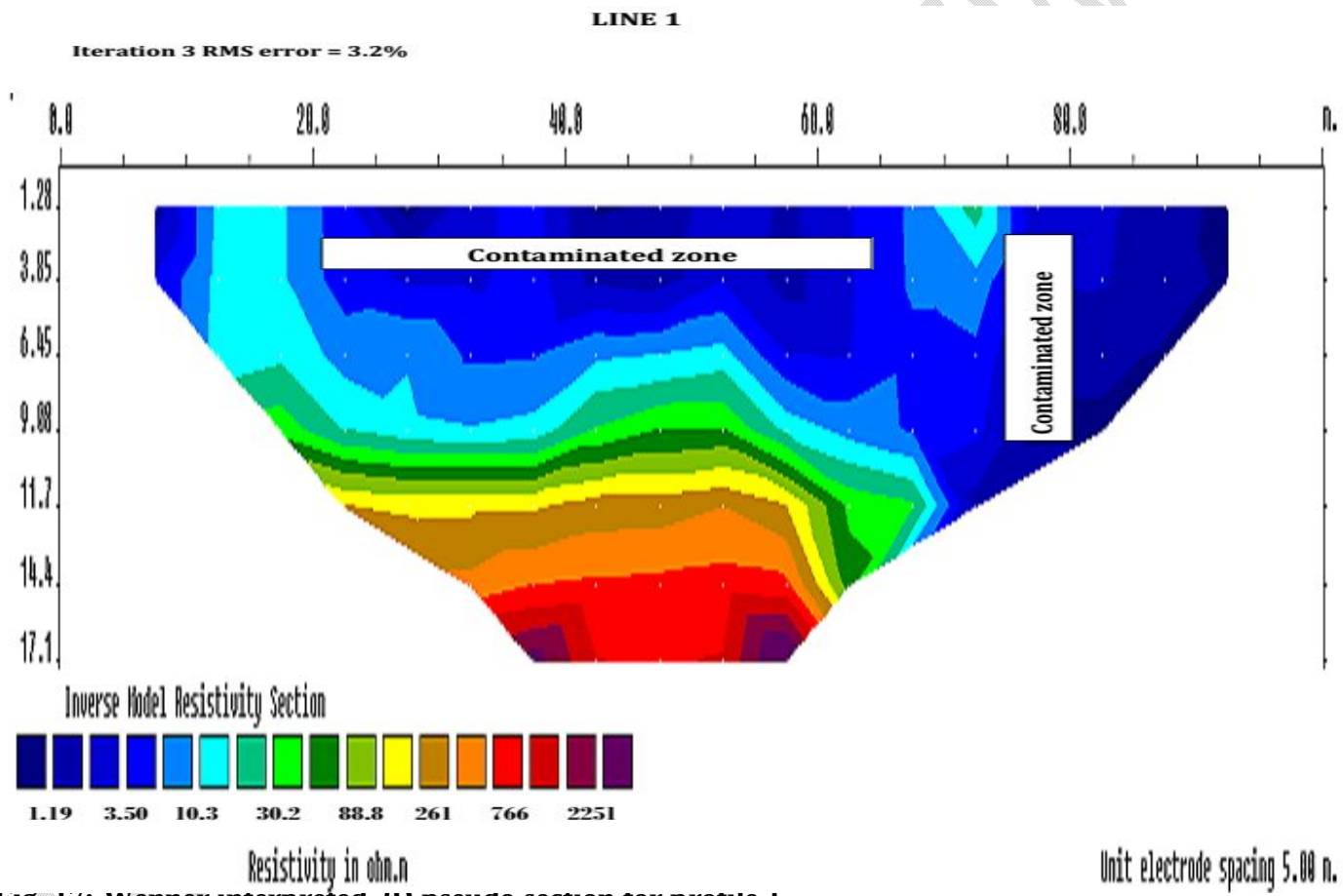


**Fig. 17: Wenner interpreted 2D pseudo section for profile 1**

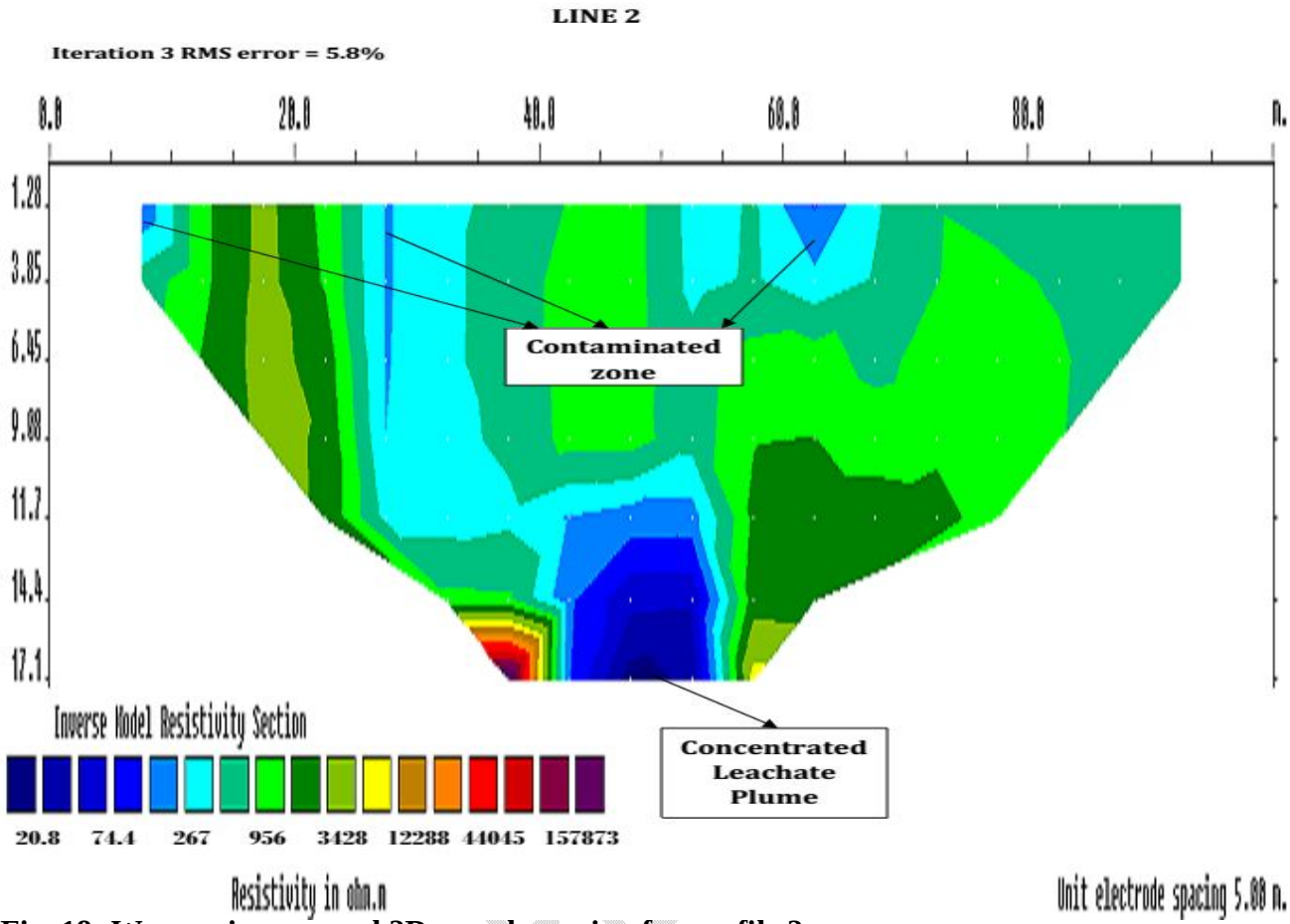


**Fig. 18: Wenner interpreted 2D pseudo section for profile 2**

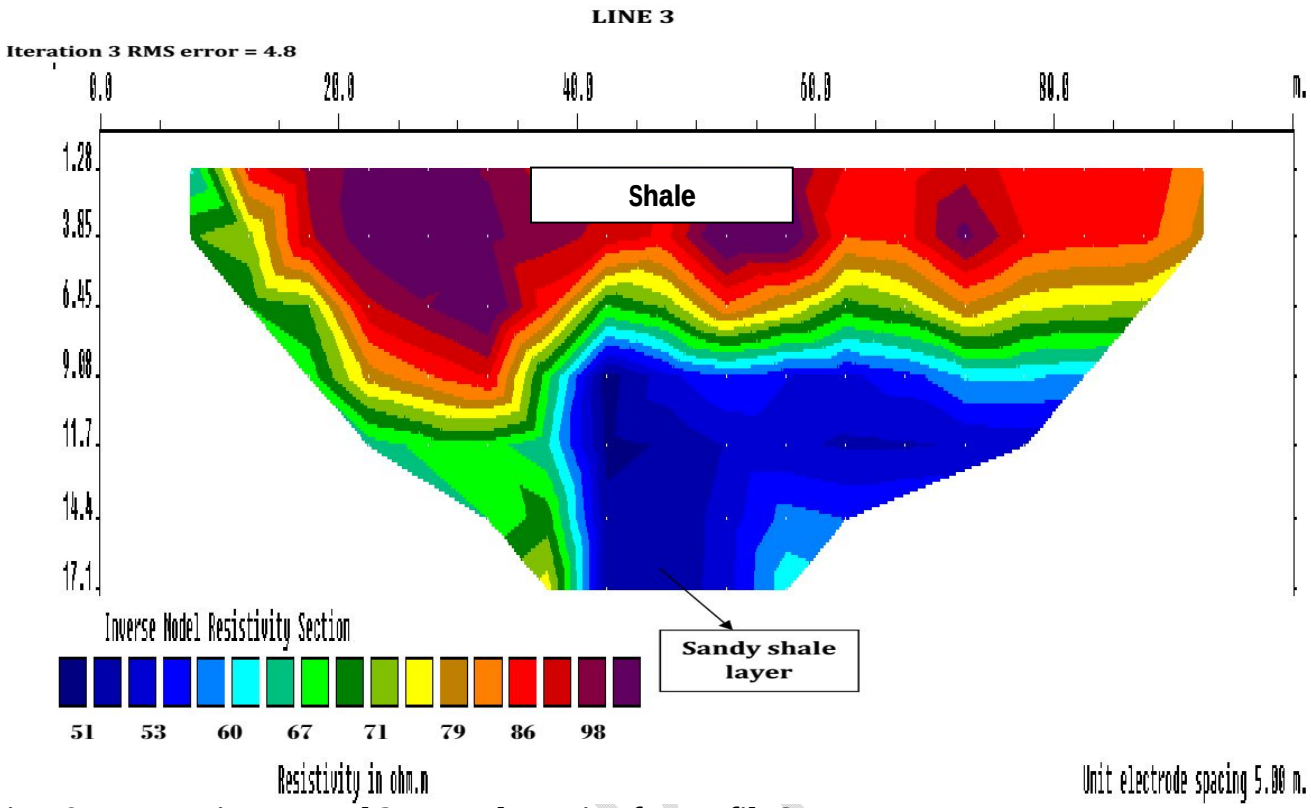


**Fig. 19: Wenner interpreted 2D pseudo section for profile 3**

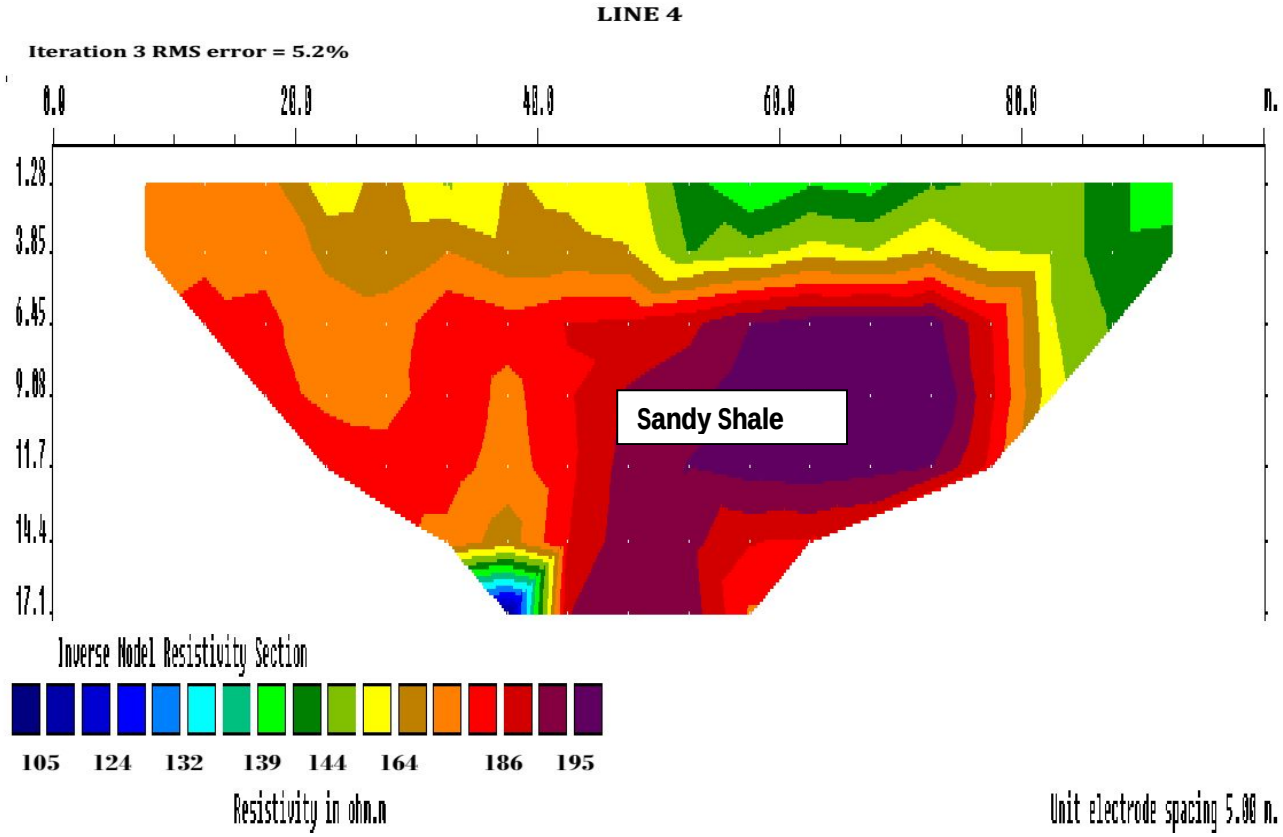


**Fig. 20: Wenner interpreted 2D pseudo section for profile 4**

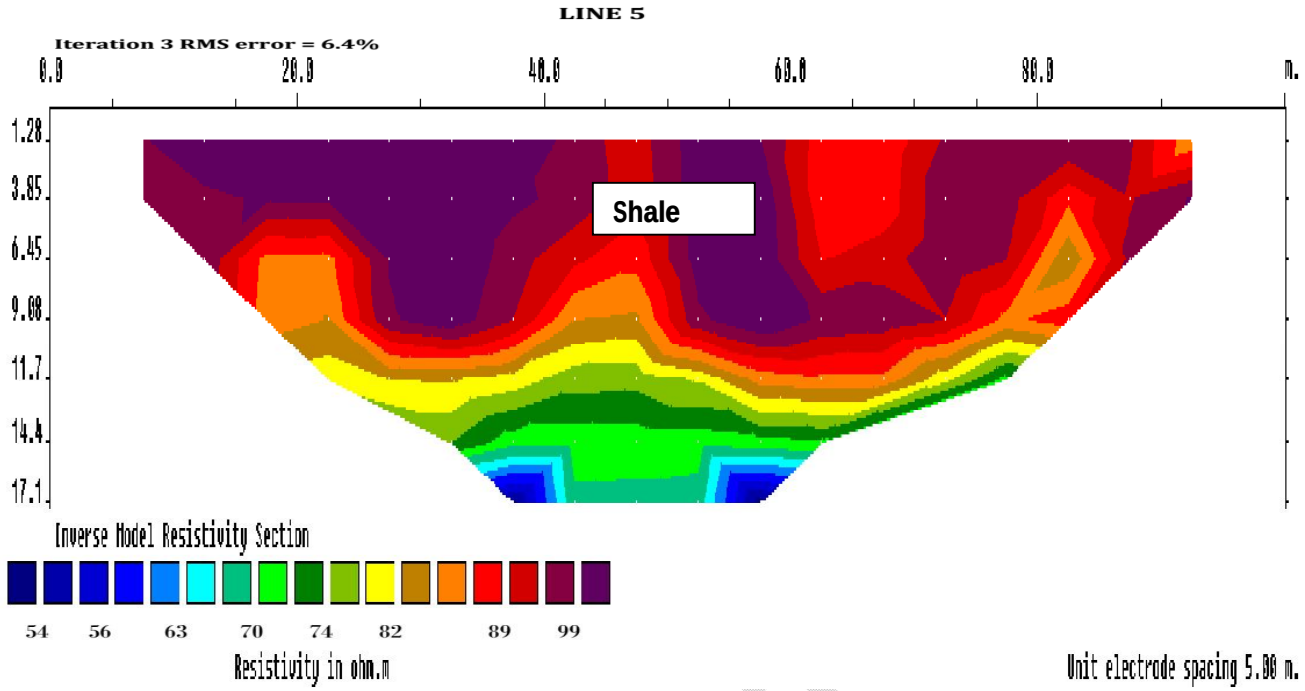


**Fig. 21: Wenner interpreted 2D pseudo section for profile 5**

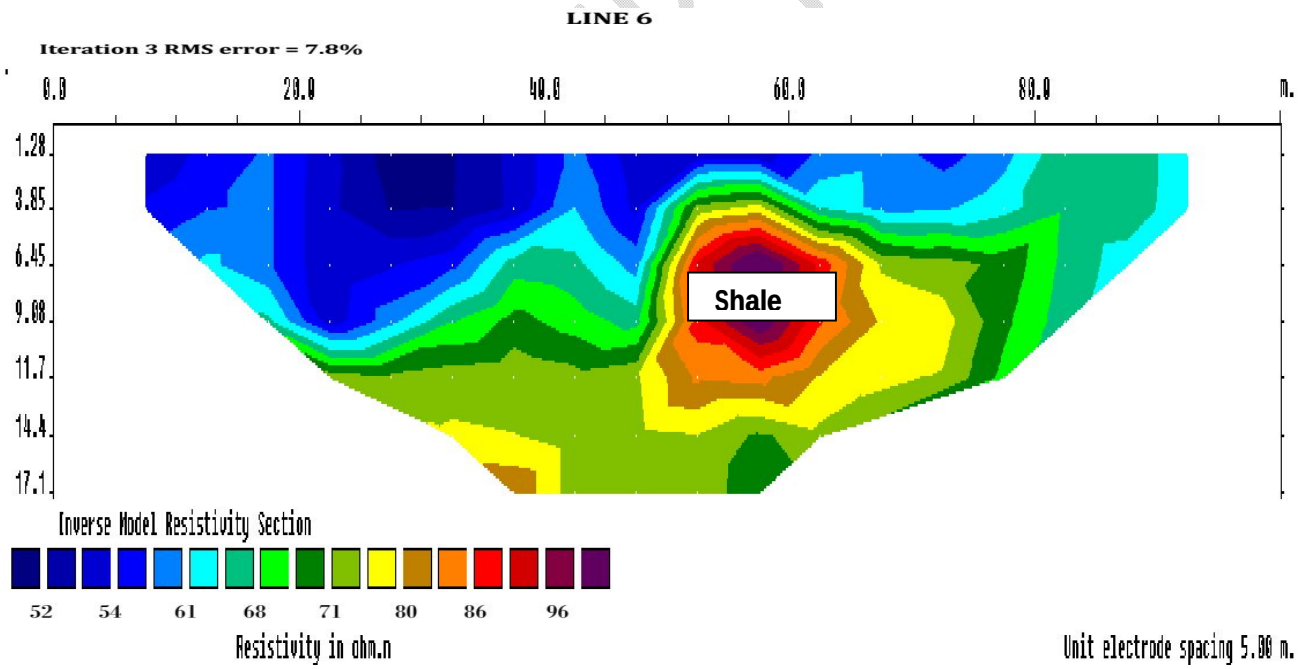


**Fig. 22: Wenner interpreted 2D pseudo section for profile 6**

**DISCUSSIONS ON THE PROFILES**

Fig. 17 – 22 shows the resistivity inversion results (iteration 3; 3.2–7.8 % total average Abs error) for profile 1 – 6 according to Cardarelli and Fischanger (2006) ;Udom*et al.* (1999) ; Nzemeka*et al.* (2023). The high range of Abs value is attributable to the small number of data points taken in the sequence of measurement in the field for building the pseudosections.

The Apparent resistivity (Ωm) is plotted against pseudo-depth (metre). The profile lines 1 – 5 runs in South to North direction and vice versa as shown in Fig 2. The Profile lines shows a maximum depth of 17.1m and lateral distance of 100m. From the surface down to approximately depth of 17.1m, there are indications of contamination as represented by low resistivity values ranging from 1.19Ωm – 20.8Ωm and indicated by the bluish colour in profile 1 - 2 (figs 17 and 18) in accordance with the result of Oyeku and Eludoyin (2010); Uma (2003); Nzemeka*et al.* (2023).

The bluish colour in profile lines 1 and 2 indicates the contaminated lateritic clay with resistivity values 1.19 – 53m while the sky bluish colour is clay soil with resistivity values ranging from 10.3 - 267Ωm respectively. From the surface down to approximately depth of 13m in profile lines 1 and 2, there are indications of contaminated or leachate plume zones as represented by low resistivity values ranging from 1.19Ωm – 10.30Ωm and indicated by the bluish colour on the section in accordance with the results of Oyeku and Eludoyin (2010); Uma (2003);Nzemeka*et al.* (2023).This contaminated zone has percolated the entire probed depth of 17.1m, where it appears concentrated in profile line 2 in fig 18. Percolation is suspected to be through pore spaces of clayey materials at the top. For profile lines 3 – 6 the bluish colour indicates the lateritic clay with depth ranging from 1.28m to 17.10m and resistivity values ranging from 51Ωm - 124Ωm with lateral distance ranging from 7.5m to 92.5m while clay soil depth ranges from 1.28m to 17.1m with lateral distance ranging from 10.0m to 80.0m.

The green and lemon colours indicates sandstone with resistivity values ranging from 30.2Ωm to 3428Ωm. Its depths ranges from 1.28m – 17.1m with lateral distance ranging from 10.8m to 86.5m in profile lines 1-3 and 20.0m to 81.5m in profile lines 4 and 6.

The yellow and brown colours indicates Ferroginized siltstone with resistivity values ranging from 80Ωm to 12888Ωm and depths ranging from 1.28m to 15.6m for profile lines 1-3 and 20.0m to 83.2m for profile lines 4 and 6. Its lateral distance ranges from 11.8m to 91.6m for profile lines 1 – 3 and 1.28m to 17.1m for profile lines 4 and 6.

The red and purplecolours indicates shale and sandy shale respectively with resistivity values ranging from 86Ωm to 44045Ωm and 96Ωmto 157873Ωm respectively with depth ranging from 14.40m to 17.1m for profile lines 1, 1.28m to 9.50m for profile line 3 and 1.28m to 17.1m for profile lines 4 and 5. Its lateral distance varies from 10.0m to 92.5m for profile line5 and 9.8m to 90.0m for profile lines 3 and 4.

Profile lines 3 – 5 does not show any evidence of contamination at the surface as captured by the resistivity values greater than 10.30Ωm in accordance with the result of Oyeku and Eludoyin (2010); Uma (2003); Nzemeka*et al.* (2023). Topographically, profile lines 3 - 5 is atop the higher plains of the gently sloping site terrain with the shale exposed at the surface.

Profile line 6 is located at the Southern end outside the dumpsite. It runs in the West to East direction as shown in fig 2. It was used as a control line in the cause of this work. Profile line 6 was carried out 100m away from the dumpsite. Subsequently, profile 6 did not show any evidence of contamination.

## CONCLUSION

A total of eight (8) Vertical Electrical Sounding (VES) using Schlumbeger array and six (6) 2D resistivity imaging using Wenner array were conducted around the dumpsite in order to determine the depth of water table, the subsurface geoelectric layers, detect and map out the contamination zones around the study area. In course of the study only line 1 & 2 are seen to be contaminated with resistivity value ranging from 1.19Ωm – 20.80Ωm and maximum depth of migration of leachate plume of 17.1m as shown in line 2. The aquiferous zone ranges from 30.26m to 155.43m. The geoelectric layers revealed litho – units as shale, clay, sand, siltstone and ferroginized siltstone

with sand being the water bearing unit. Consequently, since the depth to the aquifer ranges from 30.26m to 155.43m while maximum depth of contamination is 17.1m. It is believed that the leachate has not percolate down the aquiferous zones as such aquifers are presumed to free.

**RECOMMENDATION**

Boreholes around the study area should not be less than 30m deep to avoid exploiting polluted water. Or the screen positions of the boreholes should not be less than 30m from the surface to prevent taping water from the contaminated zones. Since dumping started in 2011 and by 2016 maximum depth of migration of the leachate is 17.1m, it is expected that in few years' time the leachate will have reached the 30m which is the minimum depth to the major aquifer in the area. Thus dumping should be discontinued to prevent future pollution of the aquifer.

**Disclaimer (Artificial intelligence)**

We hereby declare that NO generative AI technologies such as Large Language Models (ChatGPT, COPILOT, etc) and text-to-image generators have been used during writing or editing of manuscripts.

**REFERENCES**


1. Abdullahi, N.K., Udensi, E.E., Iheakanwa, A. and Eletta, B.E. (2014): Geoelectrical Method Applied to Evaluation of Groundwater Potential and Aquifer Protective Capacity of Overburden Units. *British Journal of Applied Science & Technology,* 4(14), 2024-2037.
2. Aderemi, A. O., Oriaku, A. V., Adewumi, G. A. and Otitoloju, A. A. (2011). Assessment of groundwater contamination by leachate near a municipal solid waste landfill. African Journal of Environmental Science and Technology, 5(11), 933-940.
3. Akpokodje, E.G., (1999). Principle of Applied and Environmental Geology. Paragraphic Publisher, Port Harcourt p.147.
4. Anukam LC (1997) Water pollution control—a guide to the use ofwater quality management principles case study IV—Nigeria. E& F. Spon on behalf of WHO/UNEP
5. Davis, J.L., and Annan, A.P. (1989). Ground-penetrating radar for high resolution mapping of soil and rock stratigraphy. Geophys. Prospect. 37:531–551.
6. Ezeh, C. C. (2011). Geoelectrical studies for estimating aquifer hydraulic properties in Enugu State, Nigeria. International Journal of the Physical Sciences 6 (14), 3319-3329.
7. Ezeh, C. C. and Ugwu, G. Z. (2010). Geoelectrical sounding for estimating groundwater potential in Nsukka L.G.A. Enugu State, Nigeria. International Journal of the Physical Sciences 5 (5), 415-420.
8. Han, D. M., Tong, X. X., Jin, M. G., Emily, H., Tong, C. S., & Song, X. F. (2013). Evaluation of organic contamination in urban groundwater surrounding a municipal landfill, Zhoukou, China. Environmental Monitoring & Assessment, 185(4), 3413-3444.
9. Ikhifa, I., Umego, Marius N., Obiekezie Theresa N., Egwuonwu, Gabriel N. (2017). "Geophysical Evaluation of a Landfill Site in IkpobaOkhia Local Government Area, Edo State, Nigeria" Physical Science International Journal 15(3): 1-6.
10. Kaur L, Rishi MS, Singh G, Thakur SN (2020) Groundwater potential assessment of an alluvial aquifer in Yamuna sub-basin (Panipat region) using remote sensing and GIS techniques in conjunction with analytical hierarchy process (AHP) and catastrophe theory (CT). EcolIndicat 110:105850.

11. Kadafa, A. A., Latifah, A. M., Abdullah H. S. and Sulaiman W. N. A. (2013). Current Status of Municipal Solid Waste Management Practice in FCT Abuja. Research Journal of Environmental and Earth Sciences, 5 (6); 295-304.
12. Kouzeli-Katsiri, A., Bodogianni, A. and Christoulas, D. (1999). "Prediction of leachate quality from sanitary landfill" ASCE Journal of Environmental Engineering, 125, pp. 950 – 957.
13. Kumar, R.S., Manoj D, Arvind K. N, IIT Delhi (2009) "Rating of Municipal Solid Waste Dumps and Landfills as Source of Groundwater Contamination" 97 – 108.
14. Leckie, J.O., Pacey, J.G. and Halvadakis, C. (1979). "Landfill management with moisture control". ASCE Journal of Environmental Engineering, 105, pp 337 – 355.
15. Mills, F.C. 1975. Ecological Toxicology. 3 Ed. Phenum Press London, 279p.
16. Nzemeka O. C., Ugwu G. Z. andOnyishi G. E. (2023). Groundwater potential and aquifer protective capacity at Nkwelle – Ezunaka farm estate, Southeastern Nigeria. Journal of Geology and Mining Research 15 (1): 10-24, 2023
17. Nzemeka O. C., Ugwu G. Z. andOnyishi G. E. (2023). 2D Resistivity Imaging for Leachate Migration in Nkwelle – Ezunaka farm estate, Southeastern Nigeria. African Journal of Environment and Natural Science Research 62 (2): 51-59, 2023. DOI: 10.52589/AJENSR-OIH3LABA.
18. Obiabunmo, O.C., Umego, M.N., Obiekezie T.N., Chinwuko, A. I. (2014). "Application of Electrical Resistivity Method for Groundwater Exploration in Oba and Environs, Anambra State, Nigeria". Advance in Physics Theories and Application 37; 19 – 29.
19. Olisah, N.C., Obiekezie T.N. An investigation of groundwater contamination around Nsukka municipality dumpsite using resistivity method. Scienceopen (1):22 – 33, 2020.
20. Olawale O.O., and Olayinka A.I., (2012) Very low frequency electromagnetic (VLF-EM) and electrical resistivity (ER) investigation for groundwater potential evaluation in a complex geological terrain around the Ijebu-Ode transition zone, southwestern Nigeria. JOURNAL OF GEOPHYSICS AND ENGINEERING J. Geophys. Eng. **9** (2012) 374–396
21. Onunkwo, A. A, Uzoije A.P, Darlington Ashiegbu, Cosmos C. U. (2014). Comparative Analysis of the Quality of the Shallow and Deep Aquifer Waters of Nsukka SE, Nigeria – A Preliminary Approach to Water Resource Development. Journal of Environment and Earth Science 4, (9); 25 – 34.
22. Onwe M R, Nwankwor G I, Ahiarakwem C A, Abraham EM, Emberga TT (2019) Assessment of geospatial capability index for siting waste dump/landfill to control groundwater geopollution using geographic information system (GIS) approach: case study of Abakaliki area and environs, Southeastern Nigeria. Appl Water Sci 10:12. https:// doi. org/ 10. 1007/ s13201- 019- 1087-5
23. Onwe M R, Abraham E M, Ngwu T A, Osibe K O (2022) An evaluation of the hydrogeology potential of Nsukka, Southern Nigeria, using geographic information system Applied Water Science (2022) 12:54https://doi.org/10.1007/s13201-022-01579-6
24. Pedersen, T.L 1997. UCD EXTOXNET FAQ Team. Accessed at http://extoxnet.orst.edu on 21 August, 2009.
25. Reyment, R.A. (1965). In: Aspect of the Geology of Nigeria. University of Ibadan Press: Ibadan, Nigeria. 145.
26. Singh LK, Jha MK, Chowdary VM (2018) Assessing the accuracy of GIS-based multi-criteria decision analysis approaches for mapping groundwater potential. EcolIndicat 91:24–37

27. Udom G.J., Etu – Efetor J.O., and Esu E.O., (1999). Hydrogeochemical of Groundwater in part of Port Harcourt and Tai Eleme Local Government Area, Rivers State. Global Journal of Pure and Applied Science. 5; 545 – 551.
28. Udom G.J., and Esu, E.O., (2004) A Preliminary Assessment of the Impact of Solid Wastes on Soil and Groundwater system in part of Port Harcourt City and its Environs. Rivers State Nigeria. Global Journal of Environmental Sciences 4 (1); 10 – 12.
29. Uma K.O., (2003). Hydrogeology of the perched aquifer systems in the hilly terrains of Nsukka town, Enugu State, Nigeria.Water Resources. J. NAH. 14: 85 - 92.
30. Weiss P.T., Greg LeFevre and John S. Gulliver (2008) "Contamination of Soil and Groundwater Due To Stormwater Infiltration Practices" 2 – 39.
31. Coffin ES, Reeves DM, Cassidy DP. PFAS in municipal solid waste landfills: Sources, leachate composition, chemical transformations, and future challenges. Current Opinion in Environmental Science & Health. 2023 Feb 1;31:100418.